

Supplemental Figures and Text

1. Supplementary figures

Figure S1: Efficiency of CBS and CSE inhibitor treatment, related to Figure 1.

Figure S2: CBS-deficient BMMSCs showed no alteration in adipogenic differentiation, related to Figure 2.

Figure S3: H₂S levels failed to affect adipogenic differentiation of BMMSCs, related to Figure 3.

Figure S4: Intraperitoneal injection of H₂S donor GYY4317 failed to affect adipogenic differentiation of BMMSCs in CBS^{+/-} mice, related to Figure 4.

Figure S5: H₂S level, but not homocysteine accumulation, may contribute to BMMSC impairment in CBS-deficient mice, related to Figure 5.

Figure S6: H₂S regulates Ca²⁺ influx *via* sulfhydrylation of Ca²⁺ channels, related to Figure 6.

Figure S7: Osteogenic differentiation of BMMSCs, related to Figure 7.

2. Supplementary tables

Table S1: Glossary, related to Figures 1, 3,4,5,6,7.

Table S2: *In Vivo* Used Chemical Agents, related to Figures 4, 5

3. Supplementary experimental procedures

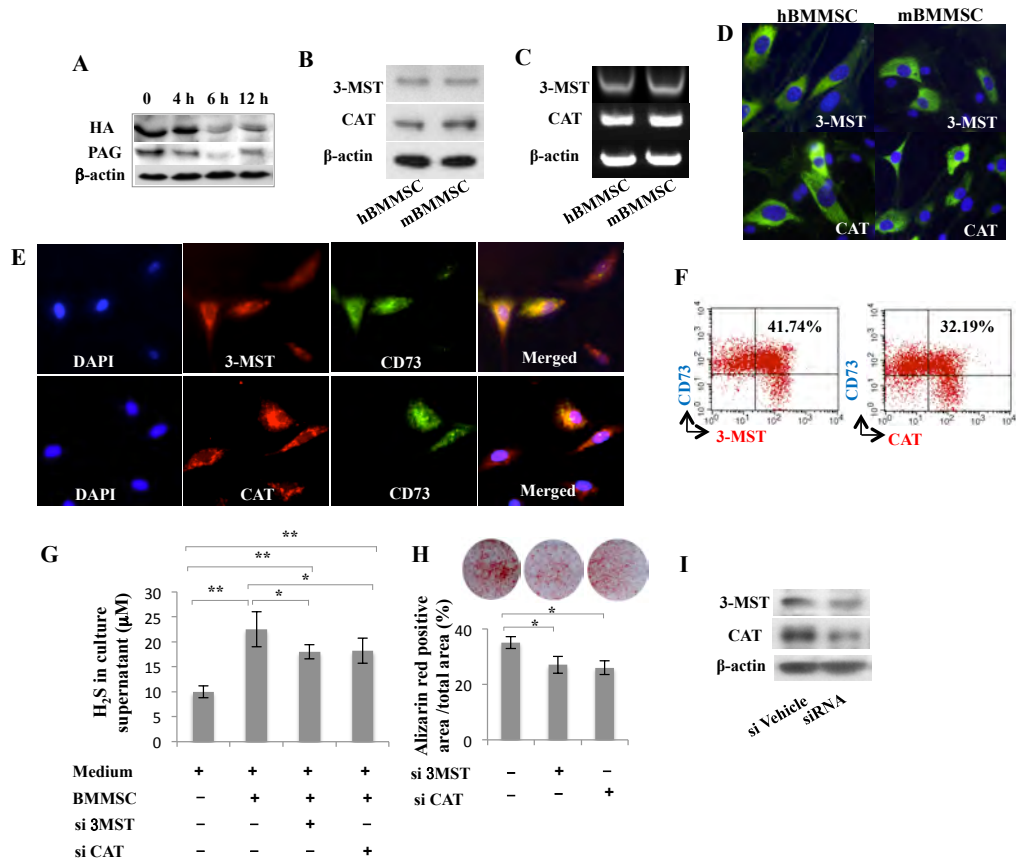


Figure S1. Related to Figure 1. **(A)** CBS inhibitor HA and CSE inhibitor PAG (100 μ M) treatment inhibited the expression levels of CBS and CSE in BMMSCs, respectively. **(B, C)** Both human (h) and mouse (m) BMMSCs express CAT and 3-MST, as assessed by Western blotting **(B)** and RT-PCR **(C)**. **(D)** Immunocytochemical staining confirmed that both human and mouse BMMSCs expressed CAT and 3-MST. **(E)** Double immunostaining showed that BMMSCs coexpressed CAT and 3-MST with the mesenchymal stem cell marker CD73. **(F)** Flow cytometric analysis showed that 32.19% of CAT-positive and 41.74% of 3-MST-positive BMMSCs expressed CD73. **(G)** H₂S produced by BMMSCs was downregulated by CAT or 3-MST siRNA treatment at 24 hours post-treatment. **(H)** Downregulation of CAT or 3-MST in BMMSCs resulted in reduced mineralized nodule formation, as assessed by alizarin red staining. **(I)** CAT and 3-MST siRNA treatment decreased the expression levels of CAT and 3-MST in BMMSCs. * $P < 0.05$, ** $P < 0.01$. Experiments were repeated three times.

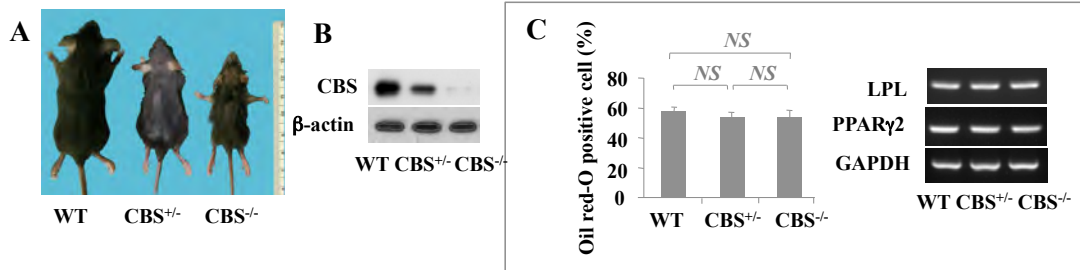


Figure S2. CBS-deficient BMSCs showed no alteration in adipogenic differentiation. Related to Figure 2. **(A)** CBS^{-/-} and 1/50 of CBS^{+/-} mice showed small size and low body weight when compared to control mice from the same C57BL6 strain (WT). Most CBS^{-/-} mice died at 4 weeks after birth. **(B)** Western blotting showed that the CBS expression level in BMSCs was decreased by about half in CBS^{+/-} mice, while no CBS expression was observed in CBS^{-/-} mice. **(C)** When cultured under adipogenic conditions, no significant difference was observed among C57BL6 WT, CBS^{+/-} and CBS^{-/-} BMSCs in terms of forming Oil red O-positive cells or expression of *LPL* and *PPARγ2*.

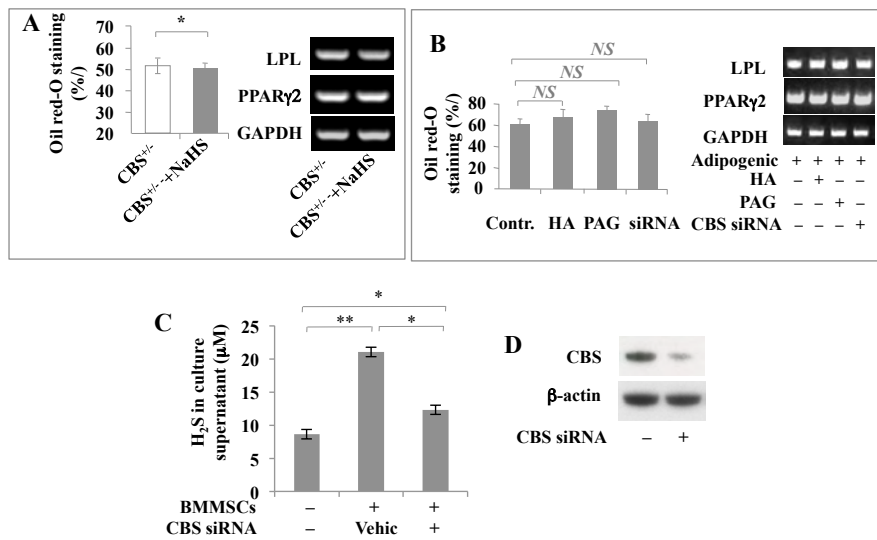


Figure S3. H₂S levels failed to affect adipogenic differentiation of BMMSCs. Related to Figure 3. **(A)** H₂S donor NaHS-treated CBS^{+/-} BMMSCs showed no alteration in adipogenic differentiation, as assessed by Oil red O-positive cell ratio and expression of adipogenic markers *LPL* and *PPAR γ 2*. **(B)** When treated with CBS inhibitor (HA), CSE inhibitor (PAG) or CBS siRNA to reduce H₂S levels, no significant change was seen in the numbers of Oil red O-positive cells or expression of adipogenic markers *LPL* and *PPAR γ 2*. **(C)** CBS siRNA was able to reduce H₂S levels. **(D)** CBS siRNA reduced CBS expression in BMMSCs. * $P < 0.05$, ** $P < 0.01$. Experiments were repeated three times.

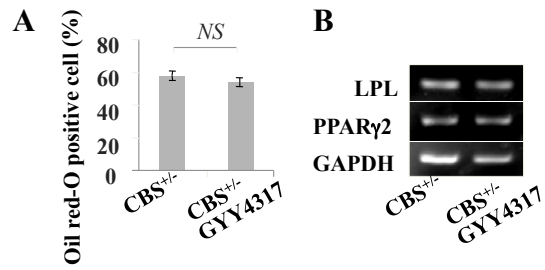


Figure S4. Intraperitoneal injection of H₂S donor GYY4317 failed to affect adipogenic differentiation of BMMSCs in CBS^{+/-} mice. Related to Figure 4. When H₂S donor GYY4317 was IP injected to CBS^{+/-} mice at 1mg/mouse/every other day for 28 days, Oil red O staining and RT-PCR showed no significant change in the number of Oil red O-positive cells (**A**) and the expression of *LPL* and *PPAR* γ 2 (**B**) between the GYY4317-treated (CBS^{+/-}+GYY4317) and untreated CBS^{+/-} groups.

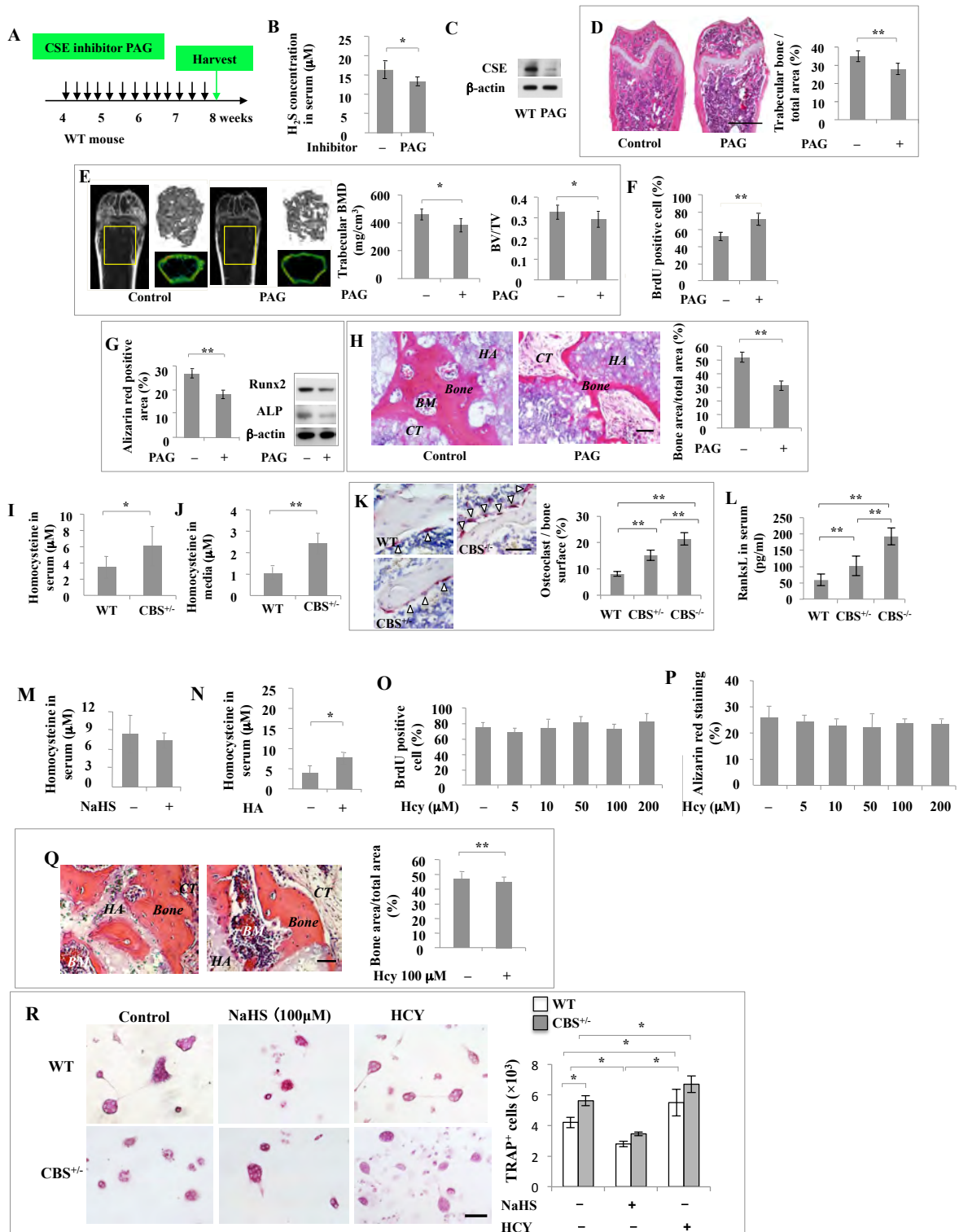
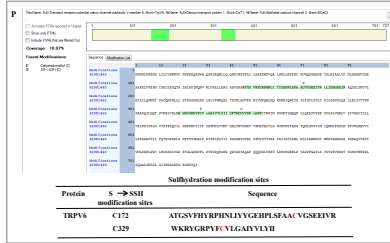
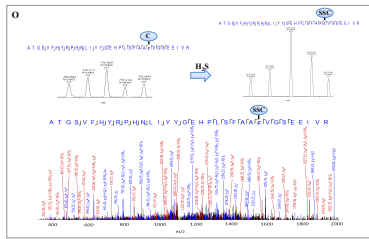
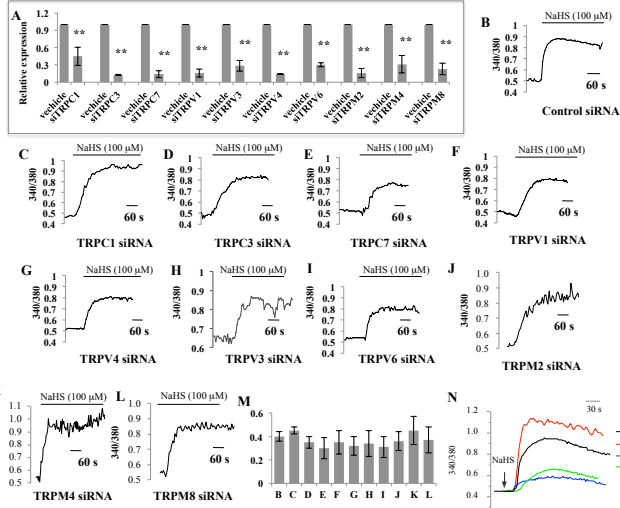


Figure S5. H_2S level, but not homocysteine accumulation, may contribute to BMMSC impairment in CBS-deficient mice. Related to Figure 5. (A) CSE inhibitor PAG was IP injected to C57BL6 mice at 100 μg /mouse/every other day for 28 days (total of 14 injections) and BMMSCs were isolated after the

last injection. **(B, C)** PAG injection resulted in significantly reduced levels of H₂S **(B)** and expression of CSE, as assessed by Western blotting **(C)**. **(D, E)** PAG injection induced marked reduction in mouse femur trabecular bone volume as assessed by H&E staining **(D)** and bone mineral density (BMD), as well as bone volume/tissue volume (BV/TV), as assessed by microQCT analysis **(E)**. **(F, G)** BMMSCs derived from PAG-treated mice showed increased proliferation rates, as assessed by BrdU labeling **(F)**, increased mineralized nodule formation, as shown by alizarin red staining, and increased expression of osteogenic markers Runx2 and ALP, as shown by Western blotting **(G)**. **(H)** BMMSCs from PAG-treated mice showed a decreased capacity to generate new bone when implanted into immunocompromised mice subcutaneously using HA/TCP (*HA*) as a carrier. *BM*: bone marrow; *CT*: connective tissue. **(I, J)** Homocysteine levels increased nearly two-fold in CBS^{+/-} mouse serum **(I)** and CBS^{+/-} BMMSC culture supernatant **(J)** in comparison to WT C57BL6 mouse serum and BMMSC culture supernatant, respectively. **(K, L)** In comparison to normal control mice, both CBS^{-/-} and CBS^{+/-} mice showed an increased number of tartrate-resistant acid phosphatase (TRAP) positive osteoclasts in the femur **(K)** and an increased level of receptor activator of nuclear factor kappa-B ligand (RANKL) **(L)** in serum, as assessed by TRAP staining and ELISA, respectively. CBS^{-/-} mice had a higher number of TRAP-positive osteoclasts and higher levels of RANKL than CBS^{+/-} mice. **(M)** IP injection of H₂S donor NaHS failed to change the serum homocysteine levels in CBS^{+/-} mice. **(N)** After IP injection of CBS inhibitor HA, CSE inhibitor PAG, or both HA and PAG, homocysteine levels in C57BL6 mouse serum increased around two-fold compared to the untreated control group. **(O, P)** Various doses of homocysteine treatment failed to change the proliferation rate of BMMSCs, as assessed by BrdU labeling assay **(O)**, or osteogenic differentiation, as assessed by alizarin red staining **(P)**. **(Q)** When implanted into immunocompromised mice subcutaneously using HA/TCP (*HA*) as a carrier, 100 μM homocysteine treatment failed to affect BMMSC-mediated new bone formation. *BM*: bone marrow; *CT*: connective tissue. **(R)** The number of osteoclast generated from CBS^{+/-} mouse bone marrow was higher than from wildtype (WT) mice. H₂S donor (NaHS) treatment reduced the number of osteoclasts for both CBS^{+/-} and WT groups, but Hcy treatment increased the number of osteoclasts when cultured *in vitro*, as indicated by TRAP staining * *P*<0.05, ** *P*< 0.01; scale bar: 1000 μm (D), 200 μm (H), 100 μm (K, Q), 50 μm (R). Experiments were repeated three times.



Q

TRPV6^{C172ms} Alignment
 Sequence ID: kd24045 Length: 2586 Number of Matches: 1
 Range: 1 to 2586

| Score | Expect | Identities | Gaps | Strand | Frame |
|-----------------|--------|-----------------|------------|-----------|-------|
| 4793 bits(2595) | 0.00 | 2597(2598/100%) | 0(2598/0%) | Plus/Plus | |

Q0492 768 GAGAGACCCCTTCTCTTCTTCTTCTGCGCGTGTGGTGTGATGAGGAGATTTGTAGAGCTGCTCA 827
 Q8345 721 GAGAGACCCCTTCTCTTCTTCTTCTGCGCGTGTGGTGTGATGAGGAGATTTGTAGAGCTGCTCA 780

TRPV6^{C329ms} Alignment

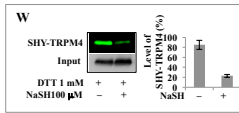
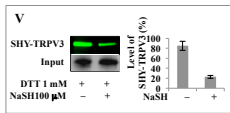
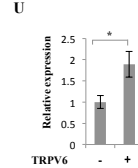
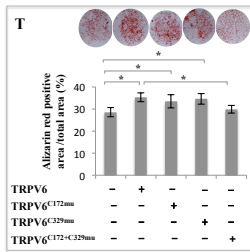
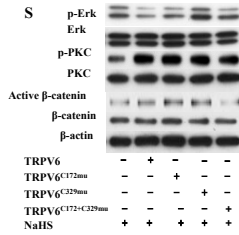
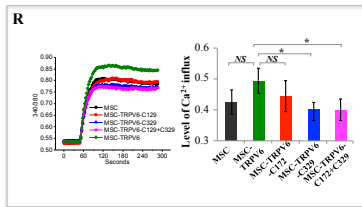
| Score | Expect | Identities | Gaps | Strand | Frame |
|-----------------|--------|-----------------|------------|-----------|-------|
| 4793 bits(2595) | 0.00 | 2597(2598/100%) | 0(2598/0%) | Plus/Plus | |

Q0414 1248 ATGSGVPHYRPNILVYGHPLSAAVVGSLEIYR 1307
 Q8345 1201 ATGSGVPHYRPNILVYGHPLSAAVVGSLEIYR 1260

TRPV6^{C172+C329ms} Alignment

| Score | Expect | Identities | Gaps | Strand | Frame |
|-----------------|--------|-----------------|------------|-----------|-------|
| 4787 bits(2592) | 0.00 | 2595(2596/100%) | 0(2596/0%) | Plus/Plus | |

Q0414 768 GAGAGACCCCTTCTCTTCTTCTTCTGCGCGTGTGGTGTGATGAGGAGATTTGTAGAGCTGCTCA 827
 Q8345 721 GAGAGACCCCTTCTCTTCTTCTTCTGCGCGTGTGGTGTGATGAGGAGATTTGTAGAGCTGCTCA 780
 Q0414 1248 ATGSGVPHYRPNILVYGHPLSAAVVGSLEIYR 1307
 Q8345 1201 ATGSGVPHYRPNILVYGHPLSAAVVGSLEIYR 1260



X Sulfhydration modification sites

| Protein | S → SSH modification sites | Sequence |
|---------|----------------------------|--|
| TRPV3 | C131 | IFAAVSEGCVEELR |
| TRPM4 | C168 | EDATQAQLPCLLVAGSGGAADCLVLETDLTAP GSGGLRGEAR |

Figure S6. H₂S regulates Ca²⁺ influx via sulfhydration of Ca²⁺ channels. Related to Figure 6. **(A)** qPCR analysis showed the efficacy of siRNA knockdown for TRPC1, TRPC3, TRPC7, TRPV1, TRPV3, TRPV4, TRPV6, TRPM2, TRPM4, and TRPM8 in BMMSCs. **(B-L)** Single TRP channel knockdown by these siRNAs failed to block H₂S donor NaHS (100 μM)-induced Ca²⁺ influx. **(M)** There was no significant difference in Ca²⁺ influx between the control siRNA group and siTRP channel groups. **(N)** When pretreated with free sulfhydryl activator DTT (1 mM, red line) or free sulfhydryl inhibitor DM (1 mM, blue line) for 15 min, DTT increased NaHS-induced Ca²⁺ influx in BMMSCs, while DM decreased NaHS-induced Ca²⁺ influx in NaHS-treated BMMSCs compared to the control group (100 μM NaHS, black line). MTSES (1 mM, green line), a nonpermanent free sulfhydryl inhibitor, also reduced NaHS-induced Ca²⁺ influx, but not as effectively as observed in the DM group. **(O)** CID MS/MS analysis showed that NaHS treatment resulted in sulfhydration of cysteine residues C172 and C329 with a high level of confidence. **(P)** Detection of precursor ions at high resolution and a nearly complete series of fragmentation ions from CID allowed the accurate sequencing and assignment of the site of modification to only one site. Integrating MS and CID MS/MS results, Protein Discoverer 1.3 automatically assigned potential modification sites at C172 and C329 with high levels of confidence. **(Q)** A site mutant plasmid at C172 and C329 was generated according to Pubmed Blast results showing the alignment of TRPV6^{C172mu}, TRPV6^{C329mu} and TRPV6^{C172+C329mu} constructs. **(R)** The TRPV6 plasmid and site mutant plasmid at C172 and C329 were transfected to BMMSCs. Ca²⁺ influx was increased after overexpression of TRPV6 (MSC-TRPV6) when compared to WT BMMSCs (MSC), however, statistically difference is not significant between the two groups. When the site mutant TRPV6 plasmids were transfected to BMMSCs, the Ca²⁺ influx was significantly decreased in the C329 mutant (MSC-TRPV6-C329) and C172/C329 double mutant (MSC-TRPV6-C172+C329) groups when compared to the TRPV6-transfected group. Ca²⁺ influx in the C172 mutant group was also reduced, but this change was not statistically significant. **(S)** Western blot showed that H₂S donor NaHS (100 μM) treatment upregulated active β-catenin and p-PKC expression along with downregulated p-Erk expression in TRPV6, TRPV6^{C172mu} and TRPV6^{C329mu} BMMSCs. However, H₂S donor NaHS treatment failed to significantly change p-Erk, p-PKC and active β-catenin expression in TRPV6^{C172+C329mu} overexpressed BMMSCs. **(T)** Alizarin red staining showed that overexpression of TRPV6, TRPV6^{C172mu} and TRPV6^{C329mu} increased mineralized nodule formation in cultured BMMSCs. However, overexpression of TRPV6^{C172+C329mu} failed to affect mineralized nodule formation in BMMSCs. **(U)** Efficiency of TRPV6 overexpression in BMMSCs was assessed by qPCR analysis. **(V, W)** Sulfhydration of TRPV3 and TRPM4 calcium channels in BMMSCs was analyzed by maleimide. The green maleimide fluorescence was reduced in TRPV3 proteins from NaHS- and DTT-treated BMMSCs. **(X)** Sulfhydration modification sites of TRP calcium channels in NaSH-treated BMMSCs were identified at C131 of TRPV3 and C168 of TRPM4 by LS-MS. Experiments were repeated three times. * *P*<0.05, ** *P*<0.01. Experiments were repeated three times.

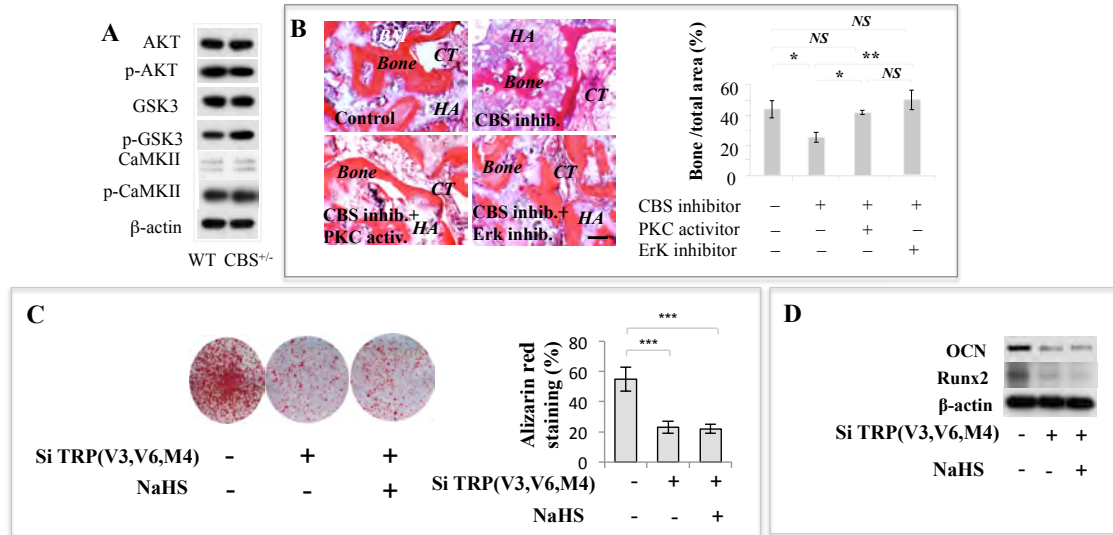


Figure S7. Osteogenic differentiation of BMMSCs. Related to Figure 7. **(A)** Expression levels of p-Akt, p-CaMKII and p-GSK3 β did not show any significant changes between CBS^{+/-} and control (WT) BMMSCs, as assessed by Western blotting. **(B)** PKC activator and Erk inhibitor treatment rescued the osteogenic deficiency in HA-treated BMMSCs, as assessed by *in vivo* BMMSC implantation to show new bone formation. HA: HA/TCP; BM: bone marrow; CT: connective tissue. **(C)** Alizarin red staining showed that combined knockdown of TRPV3, V6, and M4 by siRNA resulted in reduced mineralized nodule formation in BMMSCs, which was not rescued by NaHS treatment. **(D)** Western blot showed that knockdown of TRPV3, V6, and M4 by siRNA resulted in downregulation of the osteogenic genes osteoclastin (OCN) and Runx2, which was not rescued by NaHS treatment * $P < 0.05$, ** $P < 0.01$, *** $P < 0.001$. Scale bar: 50 μ M. Experiments were repeated three times.